PERGAMON

Continental Shelf Research 22 (2002) 899–910

CONTINENTAL SHELF RESEARCH

www.elsevier.com/locate/csr

Heavy mineral provinces of the Palos Verdes margin, southern California

Florence L. Wong*

US Geological Survey, Menlo Park, CA, USA

Received 25 March 1998; accepted 12 December 2001

Abstract

Natural sources of sediment for the Palos Verdes margin, southern California, have been augmented by effluent discharged from Los Angeles County Sanitation District's sewage-treatment facility and by the reactivation of the Portuguese Bend landslide. Heavy minerals in very fine and fine sand (63–250 μm) from beach and shelf sites off the Palos Verdes Peninsula distinguish effluent-affected sediment from unaffected deposits, and track the sediment contributed by the Portuguese Bend landslide. Heavy minerals also identify heterogeneous sediment sources for the nearshore zone and relate outer-shelf sediment to depositional cells north and south of the area. Published by Elsevier Science Ltd.

Keywords: Heavy minerals; Shelf sediment; Effluent; California

1. Introduction

Sedimentary processes in the coastal area of the Palos Verdes Peninsula, California are affected by effluent discharged from the Los Angeles County Sanitation District sewage system and by the reactivation of the Portuguese Bend landslide. Sediment samples were collected by the USGS in 1992 and 1993 as part of a multidisciplinary examination of contaminated sediment on the Palos Verdes margin (Fig. 1). The effluent-affected sediment occupies an area of $\sim 30\,km^2$ in an elongate body of 5–75 cm thick (Fig. 2; Lee et al., 2002). The sediment body typically consists of three layers: the "native" or pre-effluent sediment, the effluent-affected sediment, and surface sediment; the surface sediment contains a lower concentration of effluent (Fig. 2, inset; Lee et al., 2002). Heavy or high-density minerals were analyzed from beach and offshore sites in the Palos Verdes margin as part of the multidisciplinary study. This report discusses the spatial and temporal heavy-mineral distributions and their relation to sediment sources.

2. Previous work

The geology of the Palos Verdes Peninsula, mapped in the 1920s and 1930s by Woodring et al. (1946), is dominated by the Altamira Shale member of the Miocene Monterey Formation. The Altamira Shale (composed of a variety of sedimentary rock types interbedded with and cut by

*Fax: +1-650-329-5190.
E-mail address: fwong@usgs.gov (F.L. Wong).

0278-4343/02/$ - see front matter Published by Elsevier Science Ltd.
PII: S0278-4343(01)00110-8

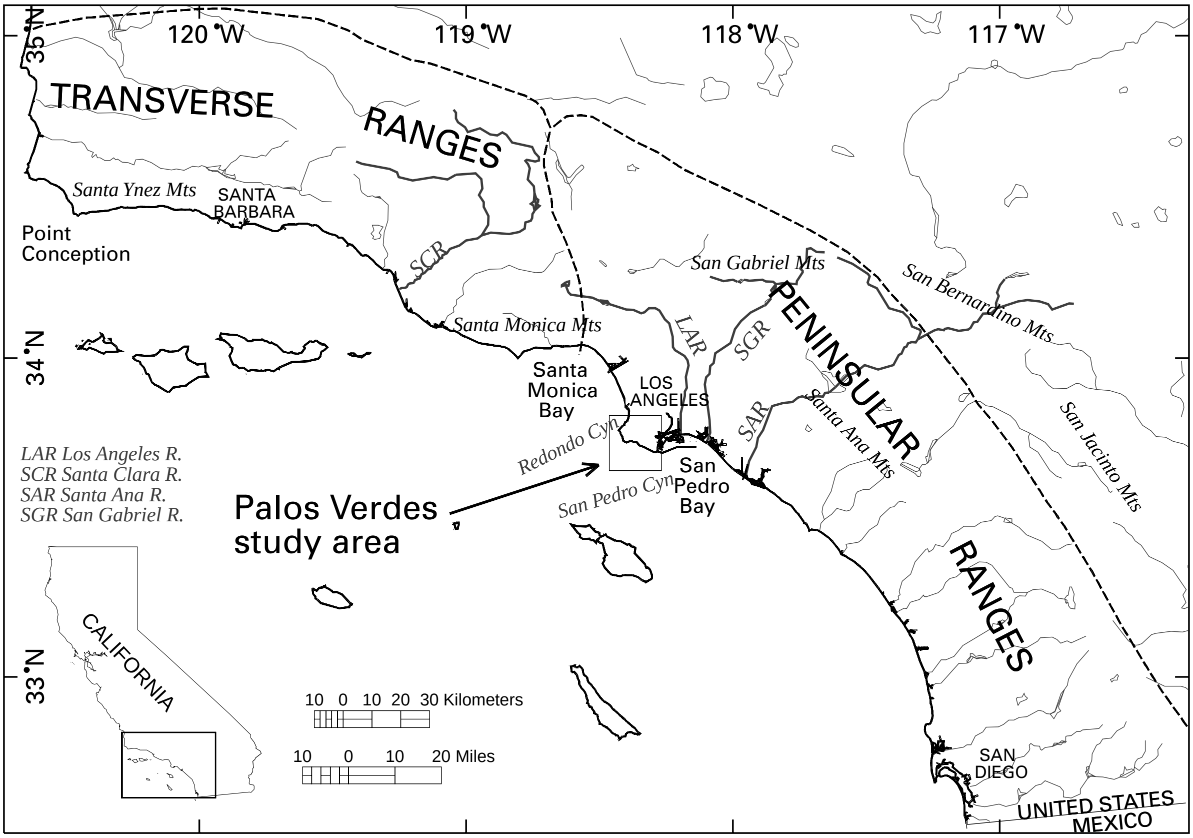

Fig. 1. Regional map of coastal southern California from Point Conception to San Diego. Several rivers near the Palos Verdes study area are highlighted for reference.

basalt sills and flows) makes up most of the southern part of the Peninsula and is exposed in the seacliffs (Woodring et al., 1946; Reiter, 1984; Schwartz and Colburn, 1987). Erosion of the Altamira Shale supplies the majority of the non-anthropogenic sediment shed to the adjacent Palos Verdes margin. The geology of this area has been studied closely since the onset of costly landslides along the southern part of the Peninsula in 1956 (e.g., Cooper, 1982; Ehlig, 1986).

More distant sources of sediment for the Palos Verdes margin have been traced to the Transverse and Peninsular Ranges of southern California (Fig. 1). The San Gabriel Mountains (part of the eastern Transverse Ranges) host the headwaters of the Santa Clara, Los Angeles, and San Gabriel Rivers. Prior to Holocene time (the last 10,000 years), those rivers carried sediment eroded from Mesozoic plutonic and metamorphic terranes in the San Gabriel Mountains to the sea both north and south of the Palos Verdes margin. During the Holocene, the sediment carried onto the margin between Point Conception and Palos Verdes has been derived more locally from sedimentary sources such as the Santa Monica Mountains and western Transverse Ranges (Rice et al., 1976; Osborne et al., 1980). In historic time, the upper reaches of the Los Angeles and San Gabriel Rivers have been confined by dams, greatly reducing their contribution of sediment to the shelf. Evidence for those sources has not disappeared from the sedimentary record because surface drainage from the Los Angeles area continues to carry similar material into sewage systems. In addition to the Los Angeles and San Gabriel Rivers, the margin southeast of Palos Verdes is supplied by other

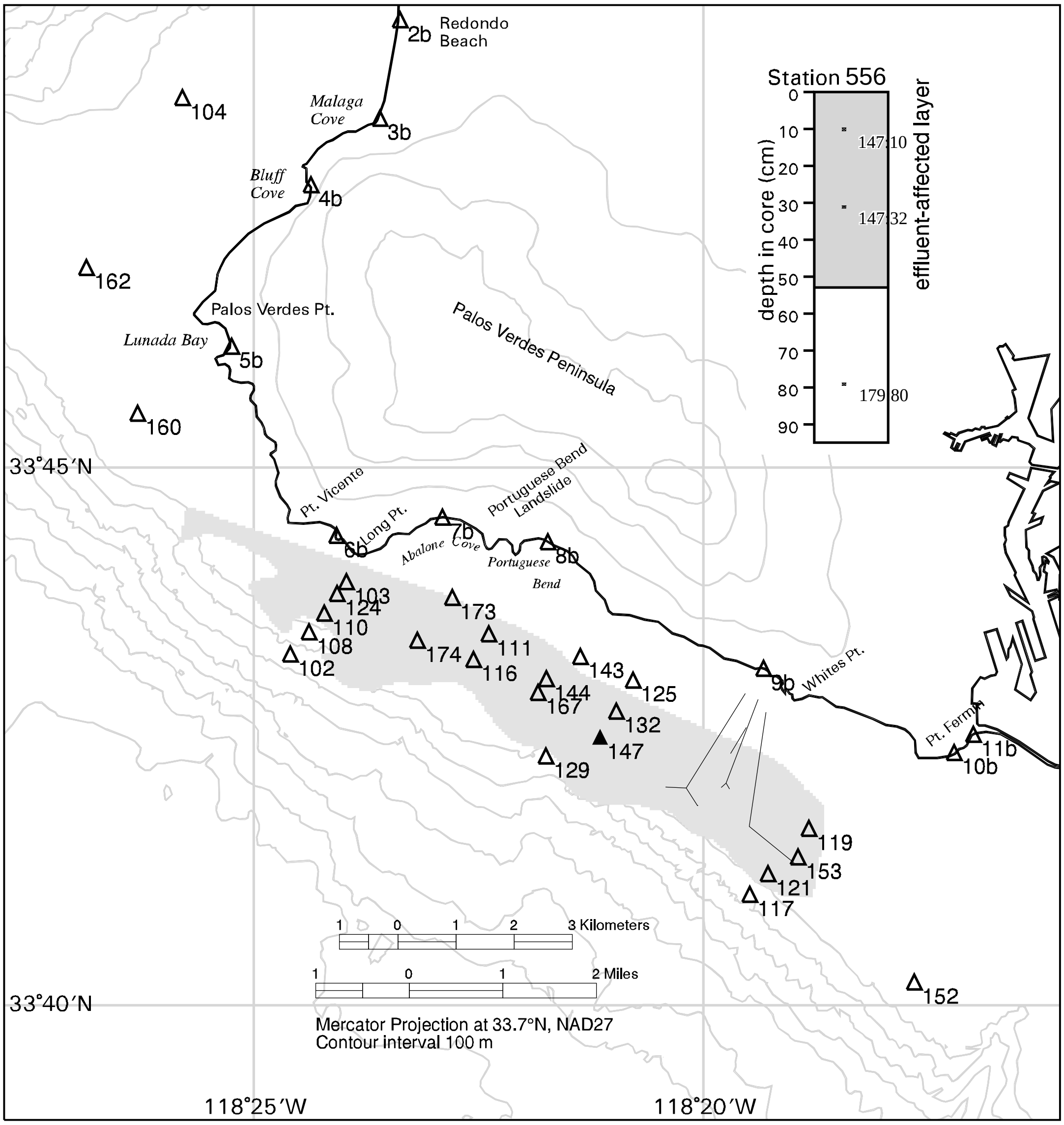

Fig. 2. Map of heavy-mineral sample sites and location names in the Palos Verdes study area. Sample numbers are centered on the sample location. The inset in the upper right is a plot of three downcore samples at station 556. Lines radiating from White's Point are the LACSD sewage diffuser pipers, which lie on the sea floor. The gray-shaded area indicates the footprint of the effluent-affected deposit thicker than 20 cm based on core data. On the station 556 inset, the gray indicates the depth of the effluent-affected deposit for that core. In core 147, the surface sediment layer, which is characterized by a reduced concentration of effluent, consists of the uppermost 30 cm. Not shown are samples 1b from Hermosa Beach north of Redondo Beach and 202 southeast of Point Fermin.

streams draining primarily plutonic rocks of the Peninsular Range (Rice et al., 1976; Osborne et al., 1980).

The sand mineralogy of the area has been studied by several workers. Rice et al. (1976) examined the mineralogy of beaches and streams from Point Conception to the US/Mexican border and determined that beach sand north of Redondo Canyon (at the northern end the Palos Verdes Peninsula) has a predominantly sedimentary rock, western Transverse Range provenance; the beach sand south of the Palos Verdes Peninsula has a dioritic provenance from the Peninsular Ranges. The Santa Clara River has headwaters in the same type of rocks as the Los Angeles and San Gabriel Rivers, but the plutonic mineralogy is diluted by the more dominant sedimentary western Transverse Ranges. Rice et al. (1976) claimed that the Palos Verdes Peninsula prevents transport of sediment between shelf areas to the north and to the south. However, Reynolds and Smith (1983) examined the mineralogy of sand samples taken from the cliff, swash, and shallow-water zones of five beaches around the Palos Verdes Peninsula and found indications that some sediment may be moving past the head of Redondo Canyon.

Reynolds (1987) examined unseparated light and heavy minerals in the very fine and fine sand fraction from samples collected from Los Angeles County Sanitation District's (LACSD) regular sampling stations on the Palos Verdes shelf as part of a sediment dynamics study. That study reported changes in sedimentation due to contributions from the introduction of effluent. The results of those studies are discussed below.

3. Sample collection

3.1. Offshore samples

Box cores (approximately $20 \times 30 \times 60\,cm^3$) were collected from shelf sites during two USGS surveys in 1992 and 1993. Several 8-cm diameter cylindrical subcores were extracted from each box core and retained for various analyses. Subsamples of 5–10 cm^3 were taken at various depths from the subcores and analyzed for textural and mineralogic content (Lee et al., 2002). Of the 27 subsamples examined in this study, 25 are from 2-cm segments in the upper 11 cm of core and are considered surface samples. For a qualitative characterization of the change in mineralogy over time, three samples are included in this study from USGS station 556: 147:10 at 9–11 cm representing the surface sediment (effluent-affected, but with a lower concentration of effluent), 147:30 at 31–33 cm representing the effluent-affected sediment, and 179:80 at 79–81 cm representing the native or pre-effluent sediment (Fig. 2: Lee et al., 2002; Kayen et al., 2002).

3.2. Beach samples

To provide a tie between offshore and onshore sediment, samples were collected from 11 beaches between Hermosa Beach in the north and Cabrillo Beach (east of Point Fermin) in the south (Fig. 2) in September 1992. For this part of the study $\sim$600–1000 cm^3 of sediment were sampled from the uppermost 10 cm of the wave-swept (swash) zone of each beach.

4. Sample preparation and analysis

Heavy minerals were separated from the 63–250-μm size fraction in tetrabromoethane (specific gravity of the heavy liquid ranged from 2.91 to 2.94). Representative splits of the grains were permanently mounted in piccolyte (refractive index = 1.52) on 27×45-mm^2 glass slides for analysis by point counting. Between 300 and 600 heavy grains were counted to insure that a statistically representative number (at least 200) of nonopaque grains were included. Grains were counted along longitudinal traverses of the grain mount. Minerals were identified by standard optical properties and, in some samples, confirmed by powder X-ray diffraction and microprobe analysis (Wong, 2001).

The abundance of each mineral was calculated as a percent of the total grains counted for each sample. The resulting percent data were processed using an in-house factor-analysis program (FA-CAN, written by M.A. Noble, USGS, 1985, last revision 1993; written communication). The factors for this study were determined using the Q-mode method. Data were first scaled using the maximum value for each mineral. The cosine–theta statistic was used as the measure of similarity. Factors were rotated using the varimax method (see Joreskog et al., 1976, for further discussion of this statistical method). After several test iterations, the final number of factors requested was nine, which accounted for 89% of the total data. Of the nine, each of factors 5, 7, 8, and 9 accounts for $<5\%$ of the data (Table 1). Details of the point-count data and factor analysis are tabulated in a separate report (Wong, 2001).

5. Mineral distributions

The distribution of the mineral percentages for the most abundant nonopaque minerals provides a general indication of the depositional provinces in the area (Fig. 3). The nonopaque heavy minerals with the greatest mean abundance are hornblende (31%), augite (14%), epidotes (9%), and barite (9%) (Wong, 2001). Carbonate fragments and glaucophane are minor constituents.

Hornblende (including brown, green, and basaltic varieties) is concentrated in samples from the outer shelf and downcore at station 556 (Fig. 3a). Abundances of 50% or more of the heavy-mineral fraction are common. Hornblende is also a common component in the shelf deposits south of Palos Verdes (Emery, 1960; Judge, 1970; Rice et al., 1976).

Augite is concentrated in the area around Abalone Cove (88%) and Portuguese Bend and offshore to about 30 m depth (Fig. 3b). Augite in these samples is a brown to reddish-brown clinopyroxene containing as much as 1.6% TiO_2 probably eroded from the basaltic volcanic rocks in the Altamira Shale (Reiter, 1984).

The distribution of epidote group minerals is similar to that for hornblende; they make up as much as 20% of the heavy-mineral fraction (Fig. 3c). Epidote, a common component of many types of rocks, is a component of shelf sediment both north and south of Palos Verdes, but is more abundant to the north (e.g., Rice et al., 1976).

Barite is concentrated near Long Point (80% of heavy-mineral fraction) and offshore Redondo Beach, and occurs in moderate amounts at White's Point (Fig. 3d). Barite probably formed as a hydrothermal-vein mineral related to basaltic intrusions located throughout the Palos Verdes area (Emery, 1960).

Carbonate fragments are abundant at Lunada Bay and White's Point beaches (Fig. 3e). These fragments are probably aragonite from disintegrating shell fragments. Glaucophane is common only at Point Fermin (Fig. 3f). Cliffs between White's Point and Point Fermin expose arenite with grains of glaucophane schist (Woodring et al., 1946; Cherven and Russell, 1987).

The mineral abundances change with depth at station 556 (Table 2). The pre-effluent sample (80 cm) is similar to that of the surface sample (10 cm) in abundances of hornblende and augite. The surface sample is richer in epidote and apatite. The mid-effluent sample (32 cm) has less hornblende and augite and more mica and carbonate fragments than the pre-effluent or surface samples. The pre-effluent and mid-effluent samples have about the same amount of epidote.

6. Factor analysis

Factor analysis statistically cross-matches mineral proportions among all the samples and produces a number of factors or associated minerals which refine the boundaries of the depositional provinces suggested by individual minerals described in the previous section (Wong, 2001). Nine factors or mineral groupings explain most (89%) of the variance in the data set (Table 1). Factors 1 and 2 together explain more than 50% of the data variance. The presence of several minor factors indicates that the Palos Verdes shelf is a heterogeneous depocenter. The factor-loading data were interpolated and contoured using a triangulated irregular network (ESRI, 1992; Fig. 4). Only factor loading values >0.2 are shaded. Mineral assemblages represented by two of the factors are widely distributed–factor 1 is characteristic of most of the Palos Verdes margin and factor 4 of the northernmost part, whereas mineral characteristics of the other factors are more restricted in area. Some of the factor distributions have an abrupt eastern boundary because only one sample (2 0 2) was taken on the shelf east of Point Fermin. In the downcore samples at station 556, only factors 1 and 6 have loadings exceeding 0.2.

Factor 1 is characterized by apatite, green hornblende, epidotes, and sphene (Fig. 4a). These minerals are common rock-forming minerals that

Table 1
Comparison of factor loading with average mineral abundance

Factor	1		2		3		4		5		6		7		8		9	
% expl	40.0		12.9		6.4		6.8		4.9		7.8		3.4		3.5		3.6	
# spls	27		8		4		4		2		9		2		2		4	
	score	mean %	score	mean %	score	mean %	score	mean %	score	mean %	score	mean %	score	mean %	score	mean %	score	mean %
Green hornblende	**0.45**	40.08	0.00	11.27	−0.02	6.53	−0.15	15.41	−0.03	5.23	**0.59**	50.52	−0.05	17.20	−0.03	26.28	−0.02	33.50
Brown hornblende	0.16	0.57	−0.07	0.03	−0.06	0.42	0.04	0.56	0.02	0.00	−0.06	0.38	−0.08	0.21	−0.11	0.29	**0.90**	1.67
Basaltic hornblende	0.15	0.09	−0.02	0.03	0.02	0.07	0.09	0.17	−0.10	0.00	−0.19	0.03	0.12	0.13	0.04	0.00	−0.03	0.07
Blue−green amphibole	−0.06	0.01	−0.02	0.00	−0.01	0.00	0.01	0.00	−0.09	0.00	0.18	0.03	−0.08	0.00	***0.53***	0.24	0.03	0.00
Tremolite	−0.11	0.11	0.02	0.03	−0.01	0.00	0.01	0.07	−0.09	0.00	***0.48***	0.31	0.01	0.00	0.09	0.29	0.01	0.00
Glaucophane	0.02	2.30	0.05	2.02	0.00	1.07	−0.05	0.73	−0.02	0.70	0.16	3.00	**0.47**	13.23	0.10	2.72	0.03	2.09
Hypersthene	0.01	0.74	0.01	0.18	−0.04	0.15	**0.32**	3.12	0.03	0.00	−0.07	0.10	−0.06	0.25	0.08	0.10	0.07	0.90
Enstatite	0.04	0.02	−0.01	0.00	0.14	0.21	−0.12	0.00	−0.19	0.00	−0.09	0.00	0.06	0.00	0.14	0.00	***0.30***	0.21
Titanaugite	−0.07	10.45	**0.98**	47.44	−0.04	11.97	−0.01	7.57	−0.02	10.21	−0.02	9.31	−0.04	12.21	−0.03	5.32	0.05	8.28
Other clinopyroxene	0.07	2.45	0.08	2.04	−0.02	1.74	0.06	4.60	−0.01	0.70	−0.04	1.47	0.00	2.99	**0.66**	9.28	0.08	2.75
Epidote	**0.47**	12.13	0.09	4.65	0.08	4.75	0.18	12.50	0.13	2.75	0.12	11.37	−0.08	6.65	−0.09	7.21	0.02	9.94
Lawsonite	−0.01	0.18	−0.01	0.16	−0.01	0.21	−0.02	0.00	−0.03	0.00	0.04	0.24	**0.41**	3.52	−0.01	0.00	0.07	0.36
Pumpellyite	−0.03	0.00	−0.02	0.00	−0.01	0.00	0.01	0.00	−0.02	0.00	0.01	0.00	**0.37**	0.52	−0.02	0.00	0.00	0.00
Zircon	−0.06	0.29	0.00	0.07	0.06	0.27	**0.47**	1.97	−0.08	0.00	0.02	0.19	0.07	0.30	−0.01	0.44	0.00	0.29
Sphene	**0.44**	3.85	0.01	1.19	0.13	1.62	**0.25**	4.97	−0.03	0.41	−0.06	3.16	−0.10	2.48	0.04	2.23	−0.20	2.97
Garnet	−0.01	0.95	0.01	0.26	−0.03	0.30	**0.49**	3.34	0.05	0.28	0.08	0.73	−0.08	0.18	0.00	0.62	0.02	0.87
Tourmaline	0.00	0.00	−0.06	0.00	−0.08	0.00	−0.03	0.00	***0.41***	0.14	−0.05	0.00	−0.10	0.00	***0.40***	0.10	−0.06	0.00
Micas	−0.01	2.07	0.00	0.54	0.00	0.36	0.02	0.47	0.06	0.27	**0.36**	4.31	−0.01	0.65	−0.11	0.83	0.00	2.12
Corundum	0.01	0.09	−0.02	0.00	−0.01	0.00	−0.05	0.00	0.01	0.00	0.15	0.25	0.05	0.09	−0.04	0.00	−0.01	0.00
Rutile	−0.10	0.01	−0.01	0.00	−0.01	0.00	***0.49***	0.11	−0.02	0.00	0.04	0.00	0.02	0.00	−0.05	0.00	−0.02	0.00
Barite	−0.06	2.85	0.02	8.03	**0.97**	51.62	−0.04	1.67	0.05	16.09	0.00	0.47	−0.02	0.00	0.03	5.94	0.03	14.02
Apatite	**0.52**	1.72	0.05	0.59	−0.05	0.14	−0.13	1.54	−0.08	0.00	**−0.36**	0.75	0.12	1.81	0.02	0.44	−0.15	1.01
Carbonate	−0.03	1.15	0.01	4.12	−0.01	2.03	−0.02	0.27	**0.79**	33.10	−0.01	1.73	−0.02	0.34	−0.11	0.56	0.01	2.70
Altered rock fragments	0.11	8.00	0.08	6.05	0.05	5.67	0.04	7.46	**0.31**	10.47	0.03	5.75	**0.46**	21.11	0.12	8.23	0.10	8.76
Metam. Rock fragments	−0.04	0.02	−0.02	0.00	0.00	0.00	0.17	0.33	−0.04	0.00	−0.02	0.00	**0.42**	1.04	−0.06	0.00	−0.05	0.00

Notes: factor = factor number.
% expl = amount of whole data set explained by factor.
# spls = number of samples with rotated factor loading $\geqslant 0.32$.
score = rotated factor score; ***scores in bold italics*** type are high scores with very low mineral abundance; **scores** in bold type identify the characterizing minerals for each factor
mean = mean mineral abundance calculated for "# spls"
See Wong (2001) for details of factor calculation.

often occur in abundance in the heavy-mineral fraction of shelf sediment between Palos Verdes and the Mexican border (Rice et al., 1976). Rice et al. (1976) identified the dioritic San Gabriel Mountains and Peninsular Ranges of southern California as the likely source of those sediments. Factor 1 minerals, which occupy a coast-parallel band in the outer part of the Palos Verdes shelf starting from offshore Palos Verdes Point in the west, decrease shoreward. Factor 1 is probably related to regional rather than local sedimentary processes, pointing to sediment supplied by rivers into San Pedro Bay and carried northwestward to the Palos Verdes shelf. Similar sediment may be carried by urban runoff as part of the effluent that has been discharged from the diffusers. In relation to the effluent deposit, factor 1 shows high (>0.8) loadings adjacent to the end of diffuser pipes, but not all high factor 1 values are associated with the effluent body.

Factor 2 is defined solely by augite (Fig. 4b). Augite occupies a zone that spreads offshore from Abalone Cove and Portuguese Bend. This augite region probably traces the advance of the Abalone Cove and Portuguese Bend landslides; values of factor 2 decrease from maximum on the beach at the toes of the slides towards the south and east out onto the inner Palos Verdes shelf. The angular augite grains were probably eroded from basaltic sills and flows in the middle Miocene Altamira Shale, which makes up the landslide and underlies most of the Palos Verdes Peninsula (Woodring et al., 1946; Schwartz and Colburn, 1987).

Factor 3 is also defined by a single mineral, barite (Fig. 4c). Its restricted occurrence near Long Point reflects a local source, though barite occurs

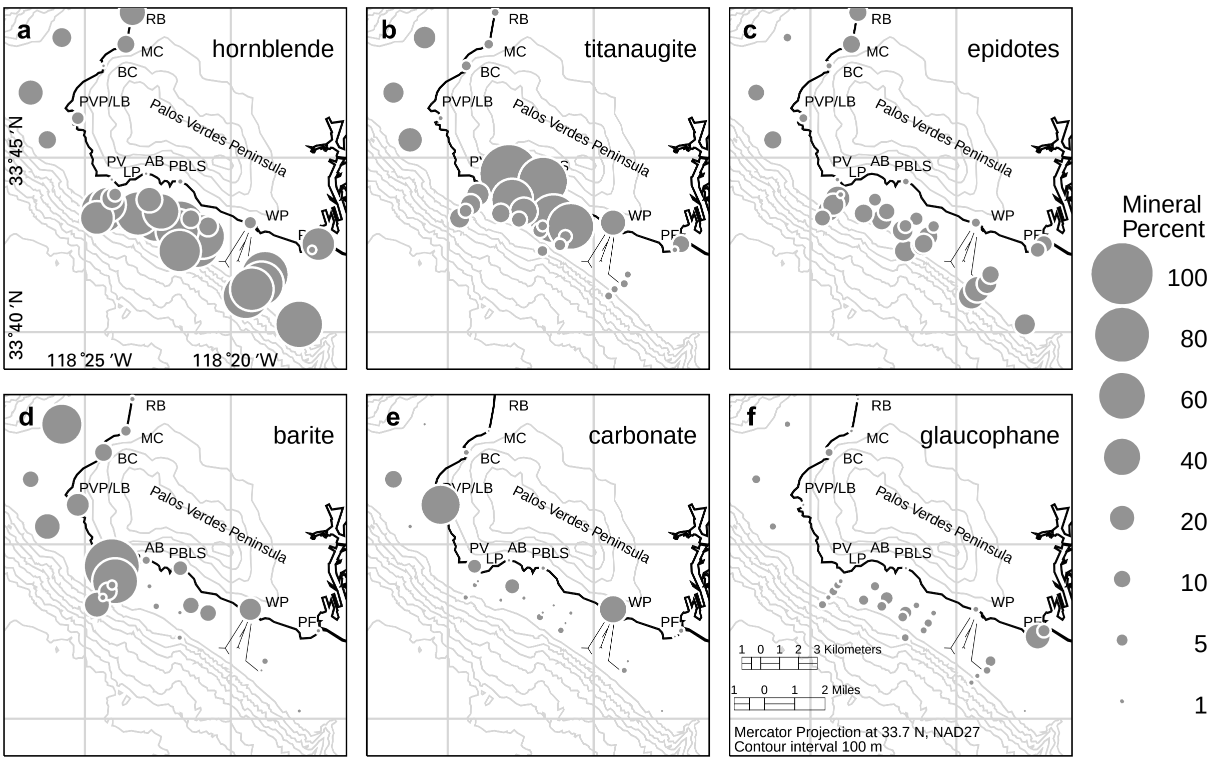

Fig. 3. Plots of mineral abundance in percent of points counted. Each spot symbol is centered on the sample location. RB Redondo Beach, MC Malaga Cove, BC Bluff Cove, PVP/LB Palos Verdes Point/Lunada Bay, PV Point Vicente, LP Long Point, AB Abalone Cove, PBLS Portuguese Bend landslide, WP White's Point, PF Point Fermin.

Table 2
Mineral abundance and factor loading of samples from station 556

Sample	147-10	147-32	179-80
Depth (cm)	9–11	31–33	79–81
Density log characteristic	Surface	Effluent-affected	Pre-effluent
Green hornblende	54.60	45.08	57.79
Brown hornblende	0.29	0.00	0.28
Basaltic hornblende	0.86	0.00	0.00
Blue-green amphibole			
Tremolite	0.00	0.27	0.00
Glaucophane	2.01	2.19	1.70
Hypersthene enstatite	0.29	0.27	0.00
Titanaugite	4.31	0.82	4.82
Other clinopyroxene	0.86	0.82	1.98
Epidote	14.37	11.20	11.33
Lawsonite	0.00	0.55	0.28
Pumpellyite			
Zircon	0.00	0.27	0.28
Sphene	5.46	3.83	2.55
Garnet	0.29	0.55	0.00
Tourmaline			
Micas	0.57	16.94	1.98
Corundum	0.00	0.27	1.98
Rutile			
Barite			
Apatite	2.30	0.82	0.85
Carbonate	0.00	3.83	1.42
Altered rock fragments	8.33	6.28	7.37
Metam. rock fragments	0.29	0.00	0.00
Loadings:			
Factor 1	0.84	0.57	0.61
Factor 6	0.11	0.60	0.46

throughout the Palos Verdes area (Emery, 1960, p. 187; Reiter, 1984, p. 52).

Factor 4 consists of garnet, zircon, hypersthene, rutile, and sphene in amounts <5% by volume (Table 1, Fig. 4d). Factor 4 has maximum values at Redondo Beach and Malaga Cove (RB and MC, Fig. 4d). Similar to factor 1, hornblende and epidotes are the most abundant minerals, but the minor minerals define this as a separate factor. The enrichment in garnet abundance makes this factor similar to that determined by Rice et al. (1976) for Santa Monica Bay rather than to the rest of the Palos Verdes margin to the south. If these samples are a blend of Palos Verdes shelf sediments and those from Santa Monica Bay, then some sediment is likely transported past the head of Redondo Canyon (upper left in Fig. 1).

Factor 5 consists of carbonate fragments and altered rock fragments; tourmaline has a high score but is present in only trace amounts (Table 1, Fig. 4e). After carbonate fragments, the most abundant minerals in the average factor 5 sample are barite and augite. The two factor 5 maxima are not connected geographically and suggest local sources of shell material that contribute to the mineral assemblage.

Factor 6 minerals lie in the midshelf area and are present downcore at station 556 (sample 147-32 and 179-80) (Fig. 4f, Table 2). The average factor 6 sample is similar to the average factor 1 sample (Table 6). Both factors 1 and 6 are dominated by the presence of green hornblende and epidotes, but the minor occurrence of micas and a smaller but persistent apatite presence (score—0.36, Table 2) separate factors 1 and 6. Factor 6 samples occupy a zone parallel to the shelf between 40 and 60 m water depth, as does much of the effluent-affected deposit (Fig. 4f).

Factor 7 consists of altered rock fragments, glaucophane, and related blueschist minerals lawsonite and pumpellyite. Sedimentary strata with grains of glaucophane schist are found throughout the Palos Verdes area. Factor 7 coincides with the exposure of the glaucophane-bearing sandstone that occurs in the cliffs between White's Point and Point Fermin (Fig. 4g; Cherven and Russell, 1987).

Factor 8 is defined by the samples from Bluff Cove and Malaga Cove and is characterized by the minor presence of clinopyroxene (other than augite) (Fig. 4h), with the most abundant minerals being hornblende and epidotes, much like those for factor 4 (Table 1).

Factor 9 is distinguished by the minor presence of brown hornblende. The maximum loading on factor 9 is from two samples on the south side of Redondo Canyon (Fig. 4i).

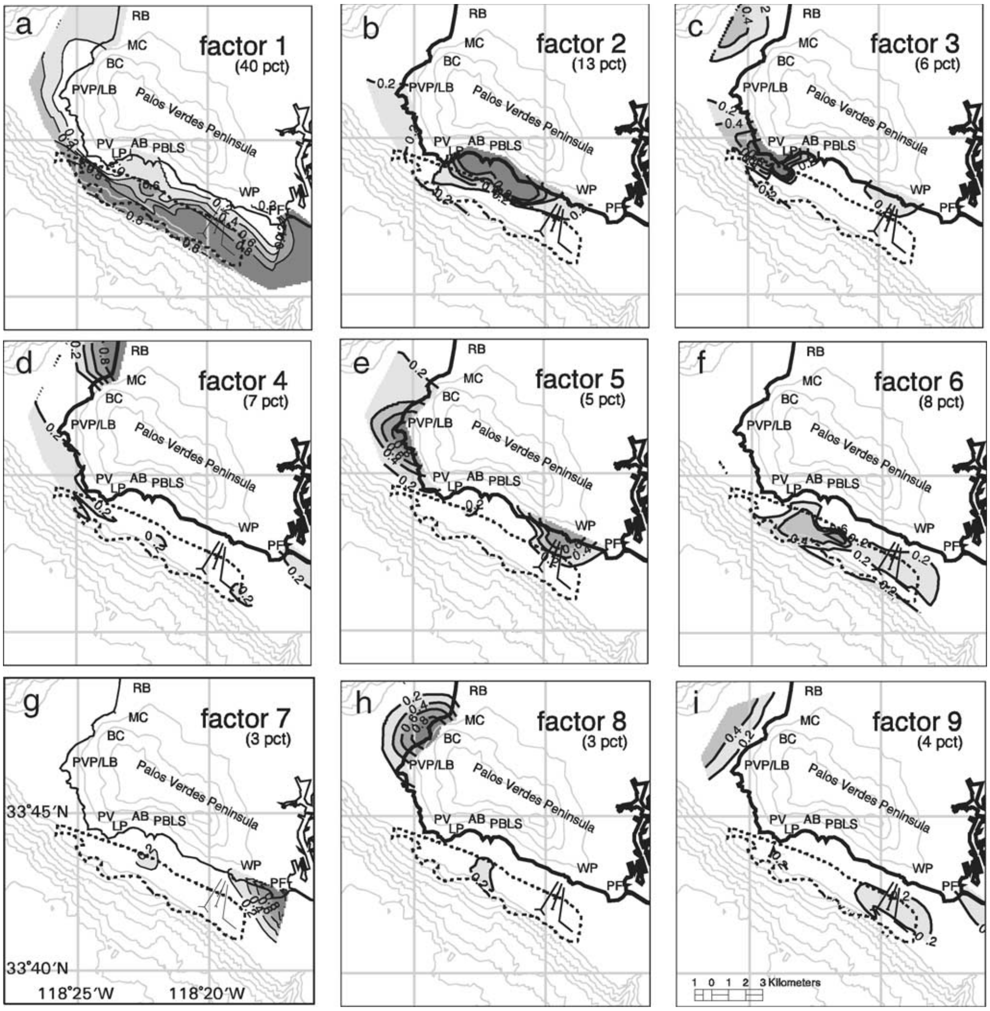

Fig. 4. Plots of factors 1 through 9 with outline of effluent-affected deposit. In panel a, for example, "40 pct" indicates that 40% of the variation in the data set is accounted for by factor 1. Locations as described in Fig. 3.

The downcore samples at station 556 provide qualitative data about the change in mineralogy before, during, and after the greatest accumulation of effluent-affected sediment (Table 2; inset, Fig. 5). Factor 1, with mineralogy characteristic of much of the shelf, is the primary component of the effluent-affected and pre-effluent samples at station 556 (147-32 and 179-80; Table 2). Factor 6 samples are absent in surface (147-10) but present in subsurface (147-32, 179-80) samples at station 556. Mineralogically, the lack of loading on factor 6 at the surface is due to the decrease in micas and increase in apatite in the surface sample. Factors 1 and 6 have comparable importance in sample 147-32 from the effluent-affected layer and the loading is slightly higher for factor 1 in sample 179-80 from the pre-effluent layer.

7. Discussion

The factor loadings that define the heavy mineral provinces of the Palos Verdes margin are combined in Fig. 5. To simplify the map, only the

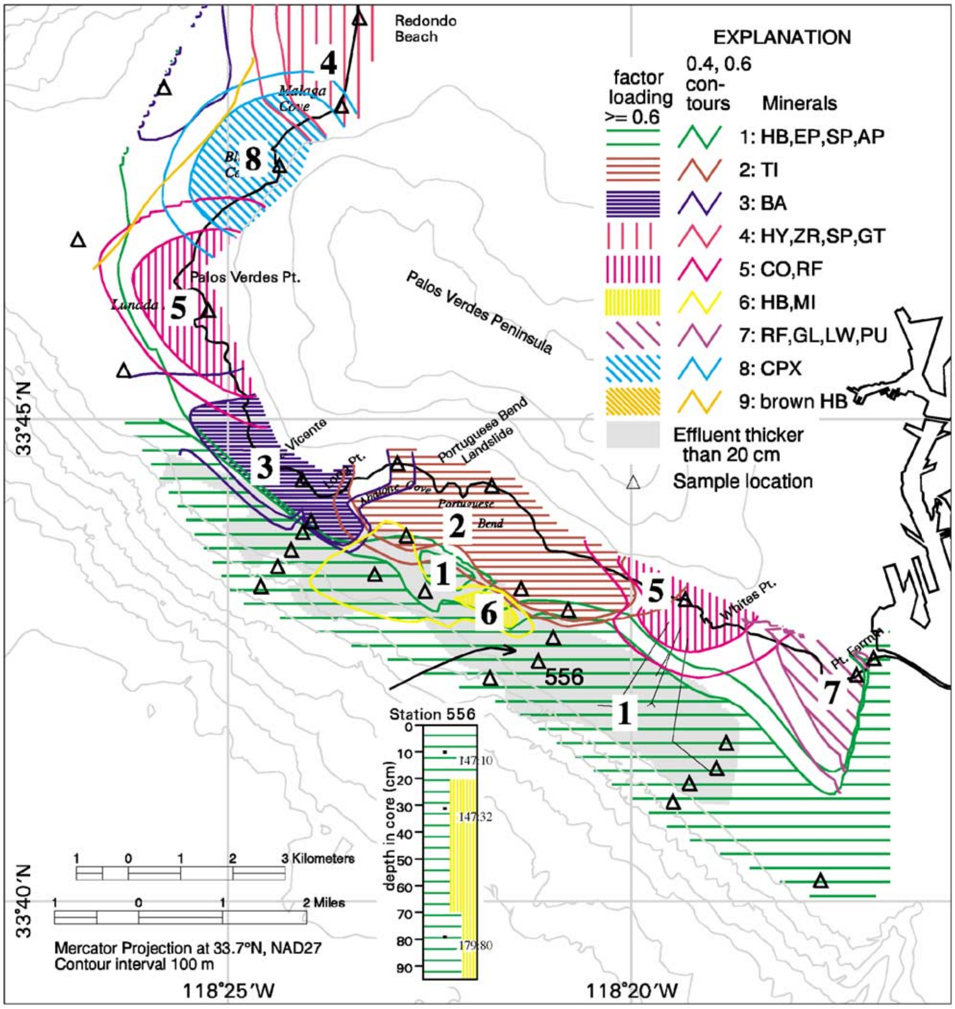

Fig. 5. Map of heavy-mineral provinces on the Palos Verdes margin. Hatchured areas have factor loadings of 0.6 or greater. Footprint of effluent-affected deposit is shaded in gray. The inset profile of station 556 is a schematic extrapolated from the three analyzed samples. Mineralogy: AP apatite, BA barite, CO carbonate, CPX clinopyroxene (excluding augite), EP epidotes, GL glaucophane, GT garnet, HB hornblende, LW lawsonite, OPX orthopyroxene, PU pumpellyite, RF rock fragments, SP sphene, TI augite, ZR zircon.

0.4 and 0.6 contours of each factor are shown, and the areas within the 0.6 contour are shaded to show the areas of highest factor loading. The 0.4 contour is included to indicate "borderline" areas. The shading was modified for the station 556 profile (inset) where the area shaded is proportional to the loading of factors 1 and 6. The influence of local sources of sediment distribution is clearly exhibited by the mutually exclusive polygons adjacent to the shoreline. The regional mineralogic signature is indicated by factor 1 for the San Pedro Bay and factor 4 for Santa Monica Bay. Each of the other factors masks those regional signatures with local contributions. This heterogeneity of local sediment sources to the beaches and nearshore Palos Verdes area has previously been noted (Reynolds and Smith, 1983). They also recognized a contribution of material from Santa Monica Bay to Malaga Cove (factor 4 in this study) and that this sediment has been transported past the head of Redondo Canyon. Rice et al. (1976) had considered the canyon an effective barrier to sediment carried south and east from Santa Monica Bay. Samples from Bluff Cove, Lunada Bay, Abalone Cove, and Point Fermin Cove each have a local or anthropogenic source of sand rather than one related to longshore transport (Reynolds and Smith, 1983).

Sediment from the Abalone Cove and Portuguese Bend landslides is traced by the distribution of factor 2 (Fig. 4b). Factor 2 within a loading value of 0.6 consists of two indistinct lobes, one trending southward from Abalone Cove that coalesces with one that trends southeastward from Portuguese Bend. At lower factor scores, traces of landslide material are seen as far west as Long Point and as far east as White's Point. The distribution is consistent with grain size data and X-ray mineralogy (Kayen et al., 2002).

The changes downcore at station 556 in factor 1 and the related factor 6 provide a means to differentiate among pre-effluent, effluent, and surface layers (Table 2). The following observations are based on only one sample at each depth and thus are necessarily qualitative. The change in mineralogy between the time the pre-effluent and effluent strata were deposited consists of a relative decrease in hornblende and augite and an increase in micas and carbonate fragments. The decrease in augite suggests a lessening of the contribution from the landslides. The increase in micas within the effluent-affected deposit may be a reflection of the decrease in grain size and sediment density; the increase in carbonate fragments may be attributed to increased biologic activity in the effluent-enriched sediment. Between the effluent-affected and surface samples, hornblende and augite increased to its pre-effluent level, epidotes and apatite increased slightly, and micas and carbonate fragments decreased to their pre-effluent level. The mineralogic changes up through the core indicate a similar sediment source through time modified by the lower-density effluent discharge. Reynolds's (1987) observed a difference in pre-outfall and present distributions of quartz varieties attributable to the Portuguese Bend landslide and to the effluent discharged by the diffuser pipes.

8. Conclusions

Heavy mineral distributions on the Palos Verdes margin indicate that the sources of sediment onshore and nearshore are heterogeneous. The outer shelf has a more uniform mineralogy that is similar to other areas between Palos Verdes and the US/Mexican border. The active Portuguese Bend landslide contributes a mineralogically distinctive volume of sediment to the shelf. The mineralogy of the shelf appears to have changed as the effluent-affected sediment accumulated.

Acknowledgements

Rob Kayen and Brian Edwards assisted in the collection of the beach samples. Valerie Coombs prepared the samples for petrographic examination. Larry Poppe and Gretchen Luepke provided helpful reviews of an earlier version of this manuscript. Jim Hein, Brian Edwards, and Raymond Ingersoll provided additional constructive reviews.

References

Cherven, V.B., Russell, P.W., 1987. Glaucophane-rich lithic sandstone at Point Fermin, California. In: Fischer, P.J. (Ed.), Geology of the Palos Verdes Peninsula and San Pedro Bay. Pacific Section, Society of Economic Paleontologists and Mineralogists, Los Angeles, CA, pp. 53–56.

Cooper, J.D. (Ed.), 1982. Landslides and Landslide Abatement, Palos Verdes Peninsula, Southern California, California. Association of Engineering Geologists, Southern California Section, Guidebook and Volume, 78th Meeting of the Cordilleran Section of the Geological Society of America, 98pp.

Ehlig, P.L. (Ed.), 1986. Landslides and Landslide Mitigation in Southern California. Guidebook and Volume, Los Angeles, California State University, 82nd Meeting of the Cordilleran Section of the Geological Society of America, pp. 151–201.

Emery, K.O., 1960, The Sea off Southern California. Wiley, New York, 205pp.

ESRI, Environmental Systems Research Institute, Inc., 1992. Surface Modeling with TIN. Environmental Systems Research Institute, Redlands, CA.

Joreskog, K.G., Klovan, J.E., Reyment, R.A., 1976. Geological Factor Analysis. Elsevier Scientific Publishing Company, Amsterdam, 178pp.

Judge, C.W., 1970, Heavy Minerals in Beach and Stream Sediments as Indicators of Shore Processes Between Monterey and Los Angeles, California. US Army Corps of Engineers, Coastal Engineering Research Center, Technical Memorandum no. 33, 44pp.

Kayen, R.E., Lee, H.J., and Hein, J.R., 2002. Influence of the Portuguese Bend Landslide on the character of the effluent-affected sediment deposit, Palos Verdes margin, southern California: Continental Shelf Research 22, 911–922.

Lee, H.J., Sherwood, C.R., Drake, D.E., Edwards, B.D., Wong, F.L., Hamer, M.R., 2002. Spatial and temporal distribution of contaminated, effluent-affected sediment on the Palos Verdes margin, southern California: Continental Shelf Research 22, 859–880.

Osborne, R.H., Scheidemann Jr., R.C., Nardin, T.R., Harper, A.S., 1980. Quaternary Stratigraphy and Depositional Environments, Santa Monica Bay, Southern California. In: Field, M.E., et al. (Eds.), Quaternary Depositional Environments of the Pacific Coast, Pacific Coast Paleogeography Symposium, Vol. 4, Pacific Section, Society of Economic Paleontologists and Mineralogists, Los Angeles, CA, pp. 143–156.

Reiter, M., 1984. The Palos Verdes Peninsula: A Geologic Guide and More. Kendall/Hunt Publishing Co., Dubuque, Dubuque, 61pp.

Reynolds, S., 1987. Sediment dynamics on the Palos Verdes Shelf. A Report submitted to the Los Angeles County Sanitation District. Supporting Materials for Data Summaries Presented at December 1, 1989 Meeting, Appendix SR(87), unpublished Report, Los Angeles, CA, 59pp.

Reynolds, S., Smith, T., 1983. Sources of sand on the Pocket Beaches of Palos Verdes Peninsula, California. Compass of Sigma Gamma Epsilon 61(1), 18–21.

Rice, R.M., Gorsline, D.S., Osborne, R.H., 1976. Relationships between sand input from rivers and the composition of sands from the Beaches of Southern California. Sedimentology 23, p. 689–703.

Schwartz, D.E., Colburn, I.P., 1987. Late tertiary to recent chronology of the Los Angeles Basin, Southern California. In: Fischer, P.J. (Ed.), Geology of the Palos Verdes Peninsula and San Pedro Bay. Pacific Section, Society of Economic Paleontologists and Mineralogists, Los Angeles, CA, pp. 5–16.

Woodring, W.P., Bramlette, M.N., Kew, W.S.W., 1946. Geology and paleontology of Palos Verdes Hills, California. US Geological Survey Professional Paper 207, 145pp.

Wong, F.L., 2001. Heavy minerals from the Palos Verdes margin, California—Data and factor analysis. US Geological Survey Open-file Report 01-153, 31p., http://geopubs.wr.usgs.gov/open-file/of01-153/.